http://www.jstage.jst.go.jp/browse/biophysics

BIOPHYSICS

Vol. 8, pp. 41–50 (2012)
doi: 10.2142/biophysics.8.41

Rigor of cell fate decision by variable p53 pulses and roles of cooperative gene expression by p53

Yohei Murakami[1] and Shoji Takada[1]

[1]*Department of Biophysics, Division of Biology, Graduate School of Science, Kyoto University, Kyoto 606-8502, Japan*

Received August 25, 2011; accepted December 28, 2011

Upon DNA damage, the cell fate decision between survival and apoptosis is largely regulated by p53-related networks. Recent experiments found a series of discrete p53 pulses in individual cells, which led to the hypothesis that the cell fate decision upon DNA damage is controlled by counting the number of p53 pulses. Under this hypothesis, Sun et al. (2009) modeled the Bax activation switch in the apoptosis signal transduction pathway that can rigorously "count" the number of uniform p53 pulses. Based on experimental evidence, here we use variable p53 pulses with Sun et al.'s model to investigate how the variability in p53 pulses affects the rigor of the cell fate decision by the pulse number. Our calculations showed that the experimentally anticipated variability in the pulse sizes reduces the rigor of the cell fate decision. In addition, we tested the roles of the cooperativity in PUMA expression by p53, finding that lower cooperativity is plausible for more rigorous cell fate decision. This is because the variability in the p53 pulse height is more amplified in PUMA expressions with more cooperative cases.

Key words: Apoptosis, cell death, computational biology, systems biology

DNA damage in cells leads to either the induction of apoptosis or activation of DNA repair and cell cycle arrest, depending on the level of DNA damage[1–3], which is termed the "cell fate decision". The precise decision is of central importance and disorder of apoptosis signal transduction often causes serious diseases such as cancer and neurodegenerative disease[4–6]. In the cell fate decision process, p53, a well-known tumor-suppressor transcription factor, plays key roles by regulating the transcription of many kinds of genes responsible for cell cycle control, DNA repair, and apoptosis induction[2,7].

Recently, it was reported that, upon DNA damage by gamma ray radiation, a series of discrete pulse-like p53 concentration changes (called p53 pulses in this article) were observed in tumor cell lines in individual cells[8–12]. It was suggested that the level of DNA damage does not severely affect the mean size or shape of each pulse, but correlates with the number of p53 pulses[10]. The p53 pulses may be generated when the level of DNA damage exceeds a particular threshold. A plausible hypothesis is that a cell "counts" the successive p53 pulses and decides the cell fate by the number of pulses[13]. In other words, the difference in the p53 pulse number elicits a different cellular response, apoptosis or survival; however, the details of the p53 pulse counting mechanism of cells and the relationship between the p53 pulse number and the cell fate decision remain largely unclear.

Currently, several studies using computational systems biology have elucidated the p53 pulse-counting mechanism and the relationship between the p53 pulse and the cell fate decision[14–21]. For example, Sun et al. (2009) modeled a Bax activation switch that counts the number of p53 pulses and decides the cell fate. In their work, the dynamics was deterministic and the p53 pulse size and shape were fixed. Thus, when the pulse number was larger than the threshold, cells always underwent apoptosis, whereas when the pulse number was below the threshold, cells always survived. The cell fate decision is completely rigorous depending on the pulse number. The threshold of the p53 pulse number that divides

Corresponding author: Yohei Murakami, Department of Biophysics, Division of Biology, Graduate School of Science, Kyoto University, Kyoto 606-8502, Japan.
e-mail: murakami@theory.biophys.kyoto-u.ac.jp

apoptosis from survival depends on their model details and kinetic parameters. Experiments suggested, however, that the pulse size and shape are variable[9,10]. More precisely, the pulse heights (also called amplitude), pulse widths, and pulse intervals (also called period) are not constants, but are variable. For example, the pulse heights of different pulses in the same cell can vary by about 3-fold[10]. This variability apparently complicates the rigorous cell fate decision. Zhang et al. (2009b) included variability in terms of the initial level of DNA damage and its repair dynamics, while the pulse size was still deterministic and fixed. The main purpose of this paper was to address the effects of variability in p53 pulses. How the variability affects the rigor of cell fate decision by counting the pulse number is investigated.

Signal transductions from p53 to the induction of apoptosis have been intensively studied and many components identified experimentally. The p53-based apoptosis signals are transmitted to mitochondria, especially to Bcl-2 family proteins that mutually interact at the mitochondrial outer membrane. Bcl-2 family proteins induce cytochrome *c* release from mitochondria to cytoplasm, and released cytochrome *c* enhances the activation of caspase in cytoplasm. Then, caspase activation turns on cascade reactions, leading to various apoptotic morphological changes[5,22]. Most of the members of Bcl-2 family proteins are known to be located at the mitochondrial outer membrane and interact with each other. Bcl-2 family proteins can be classified into 3 groups, (1) pro-apoptotic Bcl-2 family proteins (Bax etc), (2) anti-apoptotic Bcl-2 family proteins (Bcl-2, Mcl-1 etc), (3) BH3-only proteins (PUMA, NOXA, Bid etc). BH3-only proteins can be further divided into 2 subgroups, called activator BH3-only proteins (Bid etc) and sensitizer (also called enabler) BH3-only proteins (PUMA, NOXA etc). Pro-apoptotic Bcl-2 family proteins and BH3-only proteins facilitate apoptosis, whereas anti-apoptotic Bcl-2 family proteins counteract them and facilitate survival. Interactions and balances among Bcl-2 family proteins are thought to be crucial for the precise cell death decision[23,24]. For p53 to enhance apoptosis, p53 activates the expression of several kinds of Bcl-2 family proteins[22,25]. In particular, PUMA, one of the sensitizer BH3-only proteins, is a main transcriptional target of p53 in various tissues[26–28]. In computational systems biology studies, Sun et al. (2009) suggested that the Bax activation switch can count p53 pulses through PUMA accumulation and decide the cell fate. Our modeling is largely based on the signal transduction model of Sun et al. (2009). We note that Sun et al.'s model has not been verified experimentally. To experimentally verify their suggestion, we need to observe and examine the relationship between the number of p53 pulses which are directly related to the expression of PUMA and subsequent apoptosis.

In the gene expression by p53, p53 binds to the target DNA in the tetramer form in a highly cooperative manner[29,30]. This highly cooperative binding of p53 to DNA is a source of its nonlinear nature. In the latter part of this paper, we investigate how cooperativity in PUMA expression by p53 affects the rigor of cell fate decision.

In this study, based on the modeling of Sun et al. (2009), we investigated how the variable p53 pulse size affects the rigor of cell fate decision. We explored the factors which influence the rigor of cell death decision by the apoptosis signal transduction pathway. In particular, we focused on the cooperativity of PUMA expression by p53 because a highly cooperative process is thought to be the source of its nonlinear nature and strongly influences the cell fate decision.

Methods

Model of the apoptosis signal transduction pathway

In this study, we adopted a subset of the model of the apoptosis signal transduction pathway developed by Sun et al. (2009). In particular, to focus on the probabilistic nature of the apoptosis signal transduction pathway, we selected only the core of the bifurcation module, "Bax activation switch module", from the model of Sun et al. (2009) (Fig. 1).

We briefly describe the model in Figure 1. The input stimulus for apoptosis induction in this model is p53 pulses, which is supposed to be produced by gamma ray radiation-based DNA damage. Increased p53 concentration enhances the transcription of PUMA, one of the sensitizer BH3-only proteins. The output signal for apoptosis in this model is pore formation on the mitochondrial outer membrane. The pore transports cytochrome *c* from the mitochondria to cytoplasm, and the cytoplasmic cytochrome *c* activates caspases, which then induce apoptosis. Since downstream from the pore formation is relatively straightforward, we do not in-

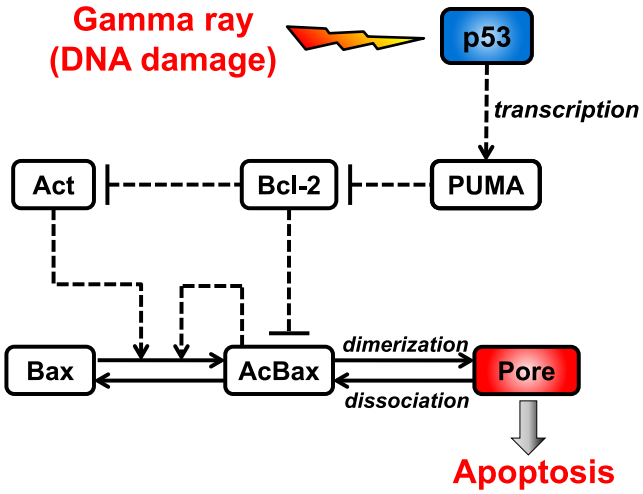

Figure 1 Schematic diagram of the model. Solid arrows represent conformational change, dimerization or dissociation of the same protein, Bax. Dotted arrow from p53 to PUMA represents enhancement of transcription. Other dotted arrows represent activation. Dotted lines with horizontal bar represent inhibition. Abbreviations: AcBax: activated Bax, Act: activator BH3-only protein.

clude it here. The pore is an oligomer (here assumed as a dimer following Sun et al. (2009)) of activated Bax, pro-apoptotic Bcl-2 family proteins. A monomeric Bax takes two forms, inactive Bax (denoted as Bax) and activated Bax (denoted as AcBax). Binding of two AcBaxs as well as binding of AcBax with Bax leads to pore formation. Activator BH3-only proteins (denoted as Act) activate Bax to form activated Bax (AcBax). Bcl-2, one of the anti-apoptotic Bcl-2 family proteins, is a key player, which binds to and sequesters activated Bax, and also inhibits Act to activate Bax. PUMA binds to Bcl-2, which reduces Bcl-2 binding to its targets, Act and AcBax. We note that PUMA expressed by p53 stimulus activates Bax not directly, but indirectly, leading to apoptosis enhancement[23,24]. In the model, all the protein interactions (all dashed lines in Fig. 1) except the arrow from p53 to PUMA are protein interactions, and the arrow from p53 to PUMA represents transcription regulation. Based on static bifurcation analysis (see *Steady state bifurcation analysis* in Results), we can unambiguously define the onset of apoptosis when the pore concentration is over 100.0 (nM) after a sufficient time (3,000 min in this work).

Model representation by ordinary differential equations, kinetic parameters and initial conditions

All protein interactions in this model are represented by ordinary differential equations following mass-action kinetics (Table 1). Only the expression process of PUMA by p53 is represented by the Hill function, as in Sun et al. (2009).

By default, we used the same kinetic parameters as in Sun et al. (2009), but changed several kinetic parameters of the expression process of PUMA by p53 based on experimental data[28,30] (Table 2). As for the maximum rate of PUMA synthesis by p53 ("*kssp53*" in Table 2), it was set 10 times higher than the PUMA basal production rate based on Yu et al. (2001). We set the Hill coefficient of PUMA expression by p53 as 2.0, by default, ("n" in Table 2) because an in vitro experiment showed that p53 binding to DNA has a Hill coefficient of 1.8[30].

In this study, for simplification, we assumed that p53 concentration is zero without DNA damage. The initial conditions of all proteins were set at the steady state concentrations when the p53 concentration was zero.

Table 1 Ordinary differential equations of the model

$$\frac{d[\mathrm{Bax}]}{dt} = ksx - kdx[\mathrm{Bax}] - kxa[\mathrm{Bax}][\mathrm{Act}] + kax[\mathrm{AcBax}] - kaxx[\mathrm{AcBax}][\mathrm{Bax}] \quad (1)$$

$$\frac{d[\mathrm{AcBax}]}{dt} = -kdax[\mathrm{AcBax}] + kxa[\mathrm{Bax}][\mathrm{Act}] - kfaxb2[\mathrm{AcBax}][\mathrm{Bcl2}] + kraxb2[\mathrm{AcBax/Bcl2}] - kfaxab2[\mathrm{AcBax}][\mathrm{Act/Bcl2}] + kraxab2[\mathrm{AcBax/Bcl2}][\mathrm{Act}] - kax[\mathrm{AcBax}] - kfaxsb2[\mathrm{AcBax}][\mathrm{PUMA/Bcl2}] + kraxsb2[\mathrm{AcBax/Bcl2}][\mathrm{PUMA}] - kaxx[\mathrm{AcBax}][\mathrm{Bax}] - 2\times kfaxax[\mathrm{AcBax}]^2 + 2\times kraxax[\mathrm{Pore}] \quad (2)$$

$$\frac{d[\mathrm{Bcl2}]}{dt} = ksb2 - kdb2[\mathrm{Bcl2}] - kfaxb2[\mathrm{AcBax}][\mathrm{Bcl2}] + kraxb2[\mathrm{AcBax/Bcl2}] - kfab2[\mathrm{Act}][\mathrm{Bcl2}] + krab2[\mathrm{Act/Bcl2}] - kfsb2[\mathrm{PUMA}][\mathrm{Bcl2}] + krsb2[\mathrm{PUMA/Bcl2}] \quad (3)$$

$$\frac{d[\mathrm{Act}]}{dt} = ksa - kda\,[\mathrm{Act}] - kfab2[\mathrm{Act}][\mathrm{Bcl2}] + krab2[\mathrm{Act/Bcl2}] + kfaxab2[\mathrm{AcBax}][\mathrm{Act/Bcl2}] - kraxab2[\mathrm{AcBax/Bcl2}][\mathrm{Act}] - kfasb2[\mathrm{Act}][\mathrm{PUMA/Bcl2}] + krasb2[\mathrm{Act/Bcl2}][\mathrm{PUMA}] \quad (4)$$

$$\frac{d[\mathrm{Act/Bcl2}]}{dt} = -kdab2[\mathrm{Act/Bcl2}] + kfab2[\mathrm{Act}][\mathrm{Bcl2}] - krab2[\mathrm{Act/Bcl2}] - kfaxab2[\mathrm{AcBax}][\mathrm{Act/Bcl2}] + kraxab2[\mathrm{AcBax/Bcl2}][\mathrm{Act}] + kfasb2[\mathrm{Act}][\mathrm{PUMA/Bcl2}] - krasb2[\mathrm{Act/Bcl2}][\mathrm{PUMA}] \quad (5)$$

$$\frac{d[\mathrm{AcBax/Bcl2}]}{dt} = -kdaxb2[\mathrm{AcBax/Bcl2}] + kfaxb2[\mathrm{AcBax}][\mathrm{Bcl2}] - kraxb2[\mathrm{AcBax/Bcl2}] + kfaxab2[\mathrm{AcBax}][\mathrm{Act/Bcl2}] - kraxab2[\mathrm{AcBax/Bcl2}][\mathrm{Act}] + kfaxsb2[\mathrm{AcBax}][\mathrm{PUMA/Bcl2}] - kraxsb2[\mathrm{AcBax/Bcl2}][\mathrm{PUMA}] \quad (6)$$

$$\frac{d[\mathrm{PUMA}]}{dt} = kss - kds[\mathrm{PUMA}] - kfsb2[\mathrm{PUMA}][\mathrm{Bcl2}] + krsb2[\mathrm{PUMA/Bcl2}] + kfasb2[\mathrm{Act}][\mathrm{PUMA/Bcl2}] - krasb2[\mathrm{Act/Bcl2}][\mathrm{PUMA}] + kfaxsb2[\mathrm{AcBax}][\mathrm{PUMA/Bcl2}] - kraxsb2[\mathrm{AcBax/Bcl2}][\mathrm{PUMA}] + stimulus \quad (7)$$

$$Stimulus = kssp53 \times \frac{[\mathrm{p53}]^n}{(Kp53)^n + [\mathrm{p53}]^n}$$

$$\frac{d[\mathrm{PUMA/Bcl2}]}{dt} = -kdsb2[\mathrm{PUMA/Bcl2}] + kfsb2[\mathrm{PUMA}][\mathrm{Bcl2}] - krsb2[\mathrm{PUMA/Bcl2}] - kfasb2[\mathrm{Act}][\mathrm{PUMA/Bcl2}] + krasb2[\mathrm{Act/Bcl2}][\mathrm{PUMA}] - kfaxsb2[\mathrm{AcBax}][\mathrm{PUMA/Bcl2}] + kraxsb2[\mathrm{AcBax/Bcl2}][\mathrm{PUMA}] \quad (8)$$

$$\frac{d[\mathrm{Pore}]}{dt} = -kdpo[\mathrm{Pore}] + kaxx[\mathrm{AcBax}][\mathrm{Bax}] + kfaxax[\mathrm{AcBax}]^2 - kraxax[\mathrm{Pore}] \quad (9)$$

p53 pulse representation

Experiments suggested that p53 pulse heights, widths and intervals do not significantly depend on the level of DNA damage, and have their own mean values as well as their own variability[9,10]. The measured mean values and standard deviations (SD) of p53 pulse widths and intervals are 350.0±160.0 (min) and 440.0±100.0 (min), respectively (mean value±SD)[10]. As for the p53 pulse heights, although the coefficient of variation (CV=SD/mean value) was experimentally estimated as 0.7[9], the mean height itself was not reliably measured. Therefore, we chose the mean height for each simulation by a certain criterion (see *Minimum pulse height for apoptosis* in Results for the details); without the variability in the pulse, apoptosis occurs after a certain number of pulses.

Instead of generating p53 pulses by the p53-Mdm2 interaction network module, here we gave the p53 pulses as Gaussian functions. Namely, the concentration of the n-th p53 pulse is represented by.

$$[\mathrm{p53}](t) = \mathrm{H} \times \exp\left(-\frac{(t - (\mu + (n-1) \times D))^2}{2\sigma^2} \right) \quad (1)$$

Table 2 Kinetic parameters of the model

Variable	Value	unit	Reference
Kp53	5.0e+2	nM	(16)
kssp53	2.0e+1	$nM \cdot min^{-1}$	(28)
n	2.0e+0	–	(30)
ksx	2.0e+1	$nM \cdot min^{-1}$	(16)
ksa	2.0e+0	$nM \cdot min^{-1}$	(16)
ksb2	6.0e+0	$nM \cdot min^{-1}$	(16)
kss	2.0e+0	$nM \cdot min^{-1}$	(16)
kdx	3.0e−2	min^{-1}	(16)
kdax	2.0e−3	min^{-1}	(16)
kda	1.0e−2	min^{-1}	(16)
kdb2	2.0e−3	min^{-1}	(16)
kdab2	2.0e−3	min^{-1}	(16)
kdaxb2	1.0e−2	min^{-1}	(16)
kds	1.0e−3	min^{-1}	(16)
kdsb2	5.0e−3	min^{-1}	(16)
kdpo	1.0e−2	min^{-1}	(16)
kxa	1.0e−4	$nM^{-1}\ min^{-1}$	(16)
kfaxb2	1.0e−3	$nM^{-1}\ min^{-1}$	(16)
kraxb2	1.0e−3	min^{-1}	(16)
kfab2	1.0e−2	$nM^{-1}\ min^{-1}$	(16)
krab2	6.0e−2	min^{-1}	(16)
kfaxab2	5.0e−4	$nM^{-1}\ min^{-1}$	(16)
kraxab2	1.0e−5	$nM^{-1}\ min^{-1}$	(16)
kax	1.0e−3	min^{-1}	(16)
kfsb2	1.0e−4	$nM^{-1}\ min^{-1}$	(16)
krsb2	1.0e−3	min^{-1}	(16)
kfasb2	5.0e−5	$nM^{-1}\ min^{-1}$	(16)
krasb2	5.0e−4	$nM^{-1}\ min^{-1}$	(16)
kfaxsb2	5.0e−4	$nM^{-1}\ min^{-1}$	(16)
kraxsb2	1.0e−2	$nM^{-1}\ min^{-1}$	(16)
kaxx	2.0e−4	$nM^{-1}\ min^{-1}$	(16)
kfaxax	2.0e−4	$nM^{-1}\ min^{-1}$	(16)
kraxax	1.0e−2	min^{-1}	(16)

Here "[p53]" is the p53 concentration (nM) at time "t" (min), "H" represents the pulse height (nM), "μ" is the peak time of the first pulse set as "pulse width/2" (min), and "σ" represents the width of the pulse set as "p53 pulse width/6" (min). Factor 6 comes from the difference in the definition of the "width". The experimentally measured "p53 pulse width" is the time difference between the onset and the end of the pulse, while σ is the "width" in Gaussian function. D represents the pulse interval (min).

To represent variable p53 pulse heights, widths, and intervals, we used random numbers. For σ, and D, random numbers were generated from the normal distribution with the above mentioned means and SDs. Pulse height was generated for the normal distribution with a given mean and SD= 0.7×mean. Figure 2 illustrates the generated p53 pulses.

Calculation of apoptosis probability

We performed 1,000 independent calculations with variable p53 pulses. The apoptosis probability is estimated as the ratio of the cases in which apoptosis occurred by the end of calculations (3,000 min).

Numerical calculation

Steady state concentrations of all proteins were calculated by solving the simultaneous equations obtained by setting all ordinary differential equations equal to zero with the standard Newton-Raphson method. Local stabilities of all steady states were determined by evaluating eigenvalues of Jacobian matrices, which were obtained by linearization of ordinary differential equations.

In the dynamics calculations, the ordinary differential equations were numerically solved by the fourth-order Runge-Kutta method with a time step of 0.01 minute.

Results

Steady state bifurcation analysis

We started with the standard steady state bifurcation analysis of the model (Fig. 3). In the figure, red and blue curves indicate stable and unstable steady states, respectively. As described above, steady states with a high pore concentration correspond to the apoptosis state, while those with

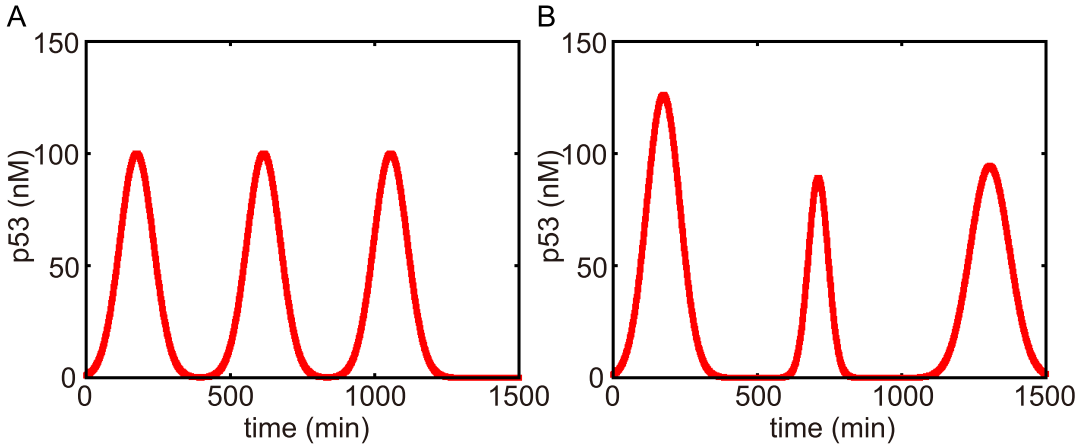

Figure 2 Examples of p53 pulses. Mean pulse height was set to 100.0 (nM) as an example. (A) An example in which the pulse heights, widths and intervals were set to constant mean values. (B) An example in which the pulse heights, widths, and interval varied.

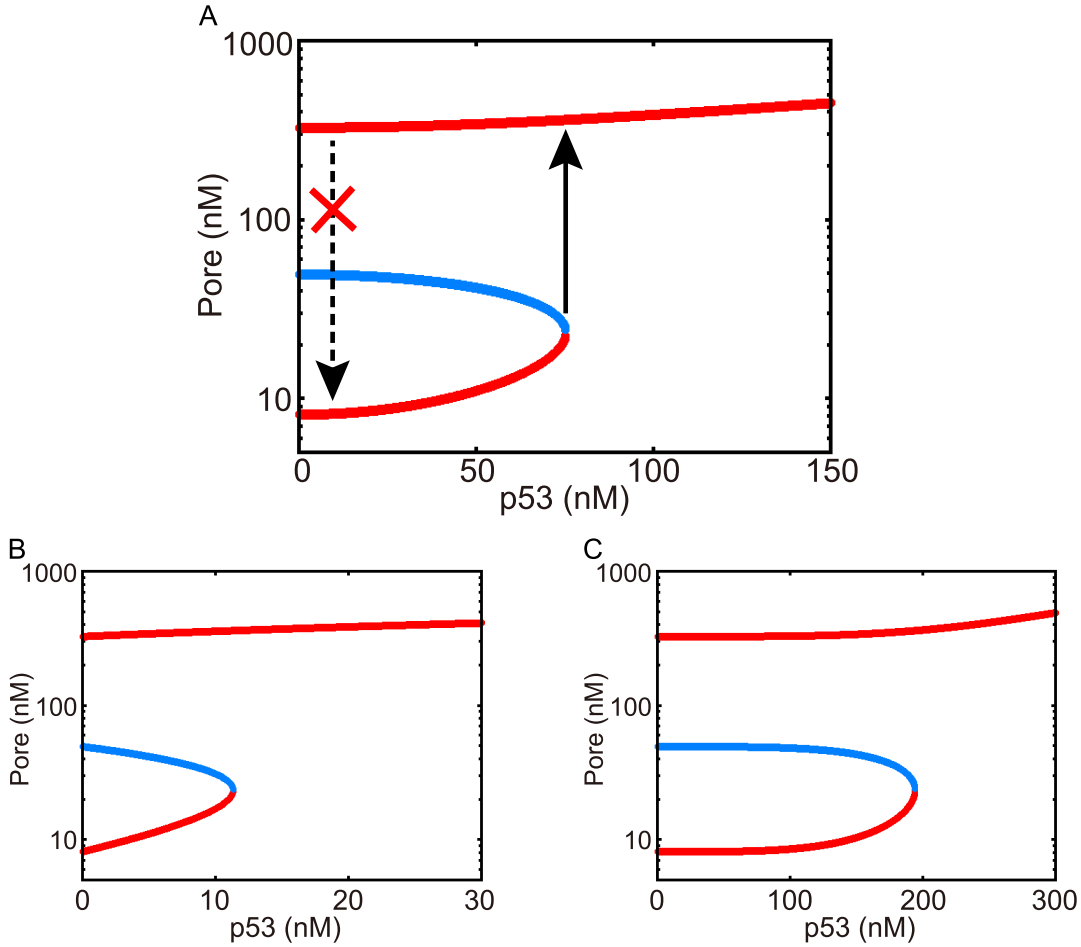

Figure 3 Bifurcation diagrams of the model system. Red curves indicate stable steady states. Blue curves indicate unstable steady states. (A) Hill coefficient = 2.0 (default value). Threshold p53 concentration (position of solid arrow) equals 75.0 (nM) (B) Hill coefficient = 1.0. Threshold p53 concentration equals 11.0 (nM) (C) Hill coefficient = 4.0. Threshold p53 concentration equals 193.0 (nM).

low (basal) pore concentration represent the survival (non-apoptosis) state. Indeed, Figure 3A shows two discrete stable states, one apoptotic and the other survival. In this bistable system, increasing the p53 concentration, the survival state suddenly disappears and abrupt transition from the survival state to the apoptosis state occurs at a threshold p53 concentration (solid arrow in Fig. 3A). Once a high level of pore is accumulated (i.e., apoptosis state), it is sustained even when the p53 concentration returns to the level below the threshold (x-marked dashed arrow in Fig. 3A). Thus, the system shows irreversibility. It has been suggested experimentally as well as computationally that the interaction network of Bcl-2 family proteins at mitochondria exhibits bistable Bax activation and pore formation[16,31–33]. In particular, two positive feedbacks, Bax auto-activation and Bcl-2 binding to activated Bax, were thought to be the origin of the bistable nature[32]. Apparently, bistability and irreversibility are important for the apoptosis signal transduction pathway to avoid improper apoptosis induced by noise, or the appearance of malignant cells by improper survival[34,35].

In this study, we address the cooperativity of PUMA expression regulation by p53, which is represented by the Hill coefficient, "n" in *Stimulus* term in Eq. (7) in Table 1. The default is n=2.0 (Fig. 3A), but we will also examine cases with n=1.0 and 4.0. Thus, we show bifurcation diagrams for n=1.0 and n=4.0 (Fig. 3B and C). As the Hill coefficient increases, the threshold p53 concentration increases, whereas the pore concentrations in the apoptosis and survival states do not alter very much. In all cases, Figures 3 robustly shows the bistability and irreversibility of pore formation by p53 concentration changes. These are essentially the same as the results in Sun et al. (2009), which dealt with more comprehensive signal transduction networks. Based on these bifurcation analyses, we set the criterion for the pore concentration in the apoptosis state as >100.0 (nM).

Minimum pulse height for apoptosis

We then performed dynamic analysis of the model. Before analyzing the roles of variability in the p53 pulses, a

Table 3 Minimum pulse height needed for apoptosis

Table 3A Hill coefficient = 1.0

p53 pulse number	p53 pulse height (nM)
1	158.0
2	88.0
3	67.0
4	57.0
5	51.0

Table 3B Hill coefficient = 2.0

p53 pulse number	p53 pulse height (nM)
1	343.0
2	254.0
3	221.0
4	203.0
5	192.0

Table 3C Hill coefficient = 4.0

p53 pulse number	p53 pulse height (nM)
1	464.0
2	394.0
3	366.0
4	351.0
5	341.0

uniform p53 pulse was examined as a control. The minimum pulse height necessary for apoptosis induction was calculated for each given pulse number (Table 3). Here, the pulse width and interval were set as 350.0 (min) and 440.0 (min), respectively, based on the above argument (see *p53 pulse representation* in Methods). As the pulse number increases, the required minimal pulse height for apoptosis induction becomes smaller. In addition, a larger pulse height is necessary for apoptosis induction as the Hill coefficient becomes larger. The calculated data of the minimum pulse height was used in the following sections to calculate the probability of apoptosis onset.

The rigor of cell fate decision and p53 pulse size variability

Now, variability was introduced into the p53 pulse size to assess how it affected the rigor of cell fate decision. Experimentally, the number of p53 pulses to induce apoptosis is unclear. In the computational study of Sun et al. (2009), with their parameter choices, the cell underwent apoptosis when the pulse was ≥3. Here, here we simply followed their model by setting the pulse height as 237.5 (nM), which is between the minimum pulse height for 2-pulse apoptosis induction and that for 3-pulse apoptosis induction (Table 3). For the pulse size variety, SDs and the coefficient of variation described in *p53 pulse representation* in Methods were used as a reference. These values are based on experiments of tumor cell lines[9,10]. It was argued that normal cells may have less variability than tumor cells[36]; therefore, based on the degree of variability in tumor cells (designed as "pulse_variability = 1"), we also tested reduced variability cases by a factor of 0.5 ("pulse_variability = 0.5"), 0.25 ("pulse_variability = 0.25"), and 0 ("pulse_variability = 0" corresponding to deterministic cases). For example, when

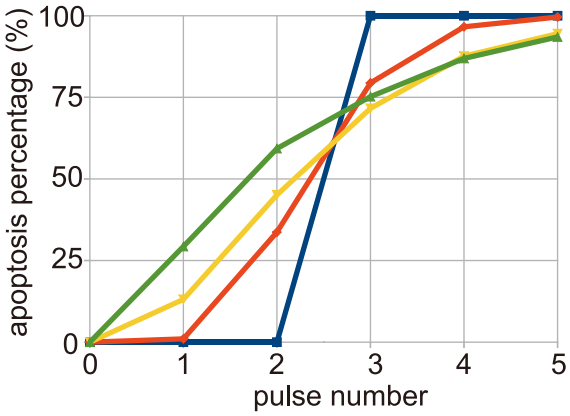

Figure 4 Apoptosis percentage (Hill coefficient = 2.0). Blue curve: pulse variability = 0.0, Red curve: pulse variability = 0.25, Yellow curve: pulse variability = 0.5, Green curve: pulse variability = 1.0.

"pulse_variability = 0.5", the SD of pulse width was set to 80.0, the SD of pulse interval was set to 50.0, and the coefficient of variation of pulse height was set to 0.35.

Figure 4 shows apoptosis probability as a function of the number of variable p53 pulses. Without variability ("pulse_variability = 0"), with our choice of pulse height, the apoptosis probability suddenly changed from 0 % for 2 pulses to 100% for 3 pulses. Due to the deterministic nature, the cell fate decision is completely rigorous. With "pulse_variability = 0.25", the cell fate decision curve softened, still showing sigmoidal behavior. As the pulse_variability increased, the sigmoidal nature was reduced, and the curves became hyperbolic. These results indicate that p53 pulse variability lowers the rigor of the cell fate decision. In normal cells, pulse height, width and interval are thought to fluctuate to some extent, as assumed in this study. With variable p53 pulse sizes, completely rigorous cell fate decision is difficult.

Recently, Zhang et al. (2009b) also investigated the variability in the cell fate decision. They investigated the stochasticity of the initial DNA damage and its repair dynamics as the source of cell fate variability, whereas the pulse size was deterministic. It is probable that variable initial DNA damage and its repair dynamics, together with intrinsic stochasticity, may induce variable p53 pulse sizes. Thus two means of variability are related, but not identical. In addition, all biochemical reactions should have intrinsic stochasticity, which further lowers the rigor of the cell fate decision. Considering these multiple sources of stochasticity will be a future study.

Role of cooperativity in the rigor of cell fate decision by variable p53 pulses

Finally, we investigated how the rigor of the cell fate decision by variable p53 pulse sizes is affected by the cooperativity in PUMA expression regulation by p53. Until this point we had used the default Hill coefficient of n=2.0, but

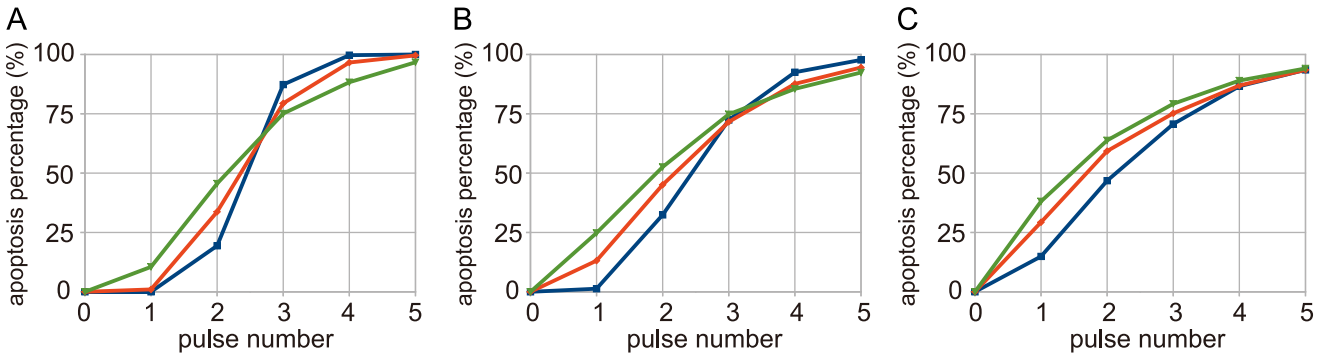

Figure 5 Difference of apoptosis percentage among different Hill coefficient systems. (A) pulse variability = 0.25. (B) pulse variability = 0.5. (C) pulse variability = 1.0. Blue curve: Hill coefficient = 1.0, Red curve: Hill coefficient = 2.0, Green curve: Hill coefficient = 4.0.

here we also used n=1.0 and 4.0. The mean pulse heights were set to 77.5 (nM) for n=1.0 and 380.0 (nM) for n=4.0, respectively, which were chosen in the same way as the default n=2.0. Figure 5 shows apoptosis probability as a function of the pulse number. Quite surprisingly, it was seen that, for the same degree of pulse variability, a larger Hill coefficient exhibits less of a sigmoidal curve. Namely, with larger cooperativity in PUMA expression regulation by p53, the cell fate decision becomes less rigorous.

Experimentally, the exact Hill coefficient for PUMA expression regulation by p53 in living cells is unclear. Weinberg et al. (2004) estimated it to be 1.8 by in vitro experiments using p53CT (residues 94–360) and synthesized DNA. Some of the earlier computational studies used n=3.0 or 4.0[16,20], probably based on the fact that p53 is a tetramer and its binding to DNA is highly cooperative[29].

Why did a larger Hill coefficient lead to a less pronounced sigmoid curve? First, it was investigated, among the three types of variability in the pulses, which variability had the largest impact on the rigor of cell fate decision. We repeated the apoptosis probability calculations, but by setting one of three SDs as zero (Fig. 6). In Figure 6, we can see that there was almost no difference among the three Hill coefficients when the pulse height was constant. In contrast, when the pulse width or pulse interval was constant, the rigor of cell fate decision seemed to depend on the Hill coefficient, similar to the Figure 5 result. These results suggest that the pulse height variability seems to be almost the sole factor influencing the rigor of cell fate decision.

Next, we tried to elucidate why pulse height variability strongly influences the rigor of cell fate decision. For example, in the case of pulse_variability = 0.5, the p53 pulse height was distributed across 154–320 nM when the Hill coefficient equaled 2.0. These ranges were input into the *Stimulus* term

$$Stimulus = kssp53 \times \frac{[p53]^n}{(Kp53)^n + [p53]^n} \qquad (2)$$

to obtain the distribution range in PUMA concentration. We show these ranges in Table 4 for different Hill coefficients ("ST range" and its width "RWS"). For better comparison, Table 4 also contains the relative ranges, the ranges divided by the mean ("NRWS"). The results in Table 4 clearly shows that, as the Hill coefficient increases, the variability in the p53 pulse height more strongly amplifies the variability in the PUMA concentration (variability in *Stimulus*), which results in the uncertainty of cell fate decision. In the current model, PUMA accumulates over p53 pulses. When the PUMA concentration exceeds a threshold, Bax activation is switched on; therefore, the cumulative amount of p53 within a certain time scale is a key factor. We calculated the cumulative amount of p53 pulses above the pore formation thresholds in Figure 3 while varying each of the three pulse characteristics (height, width and interval). Calculated averages of integrals and coefficient of variations (CV) of integrals were, respectively, 88884.88 (nM*min) and 0.25634 when the height was varied, 84848.08 (nM*min) and 0.10233 when the width was varied, and 84734.55 (nM*min) and 0.00010 when the interval was varied. These values were calculated by 1,000 simulations of 5 pulses with pulse variability = 0.5. Thus, the pulse interval is not very important. With an experimentally anticipated size of variability in pulse height and width, the height variability modulates the cumulative amount of p53 more than the pulse width.

Because of the variability amplification via the Hill formula, the apoptosis probability curves in Figure 5 become more hyperbolic with a larger Hill coefficient. Qualitatively similar results were also obtained by setting the pulse height to different values, e.g. the minimum pulse height for 3-pulse apoptosis induction (data not shown). Thus, the roles of the cooperativity of PUMA expression by p53 in the rigor of the cell fate decision found here were quite robust.

Discussion and Conclusion

We investigated how a variable p53 pulse size affects the rigor of cell fate decision, and the roles of the cooperativity in PUMA expression regulation by p53. By variable pulse sizes, the rigorous cell fate decision was disrupted. As the

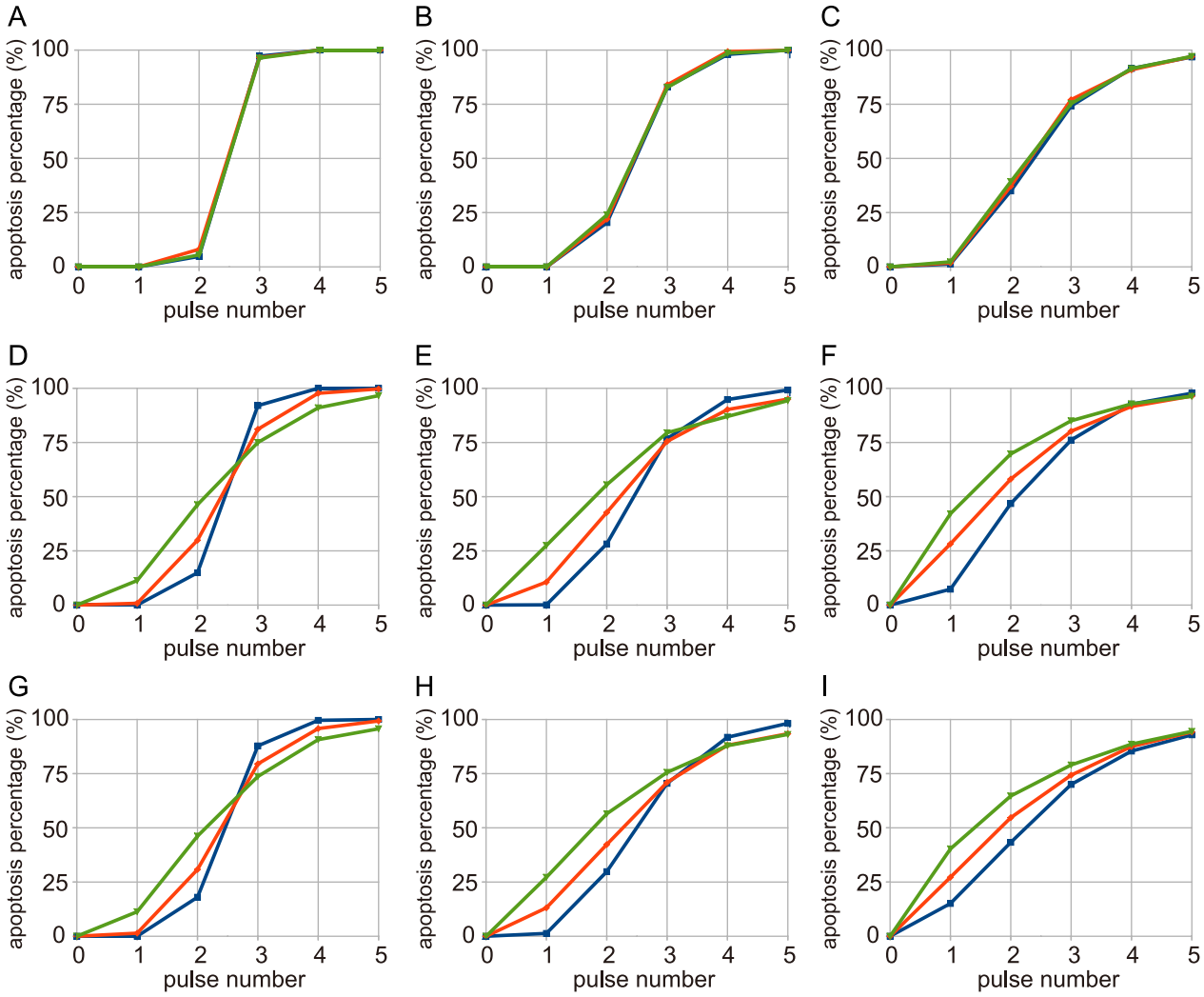

Figure 6 Apoptosis percentage with constant pulse height or pulse width or pulse interval. (A)–(C) Pulse height was set to constant value. (A) pulse variability = 0.25. (B) pulse variability = 0.5. (C) pulse variability = 1.0. (D)–(F) Pulse width was set to constant value. (D) pulse variability = 0.25. (E) pulse variability = 0.5. (F) pulse variability = 1.0. (G)–(I) Pulse interval was set to constant value. (G) pulse variability = 0.25. (H) pulse variability = 0.5. (I) pulse variability = 1.0. Blue curve: Hill coefficient = 1.0, Red curve: Hill coefficient = 2.0, Green curve: Hill coefficient = 4.0.

Table 4 Relationship between p53 concentration and the value of *Stimulus* term

Here shows pulse variability = 0.5 as an example.

HC	pulse height (nM)	ST range (nM/min)	RWS (nM/min)	NRWS
1.0	50.375–104.625	1.831– 3.461	1.630	0.607
2.0	154.375–320.625	1.741– 5.828	4.087	1.110
4.0	247.000–513.000	1.124–10.513	9.389	1.877

Abbreviations: HC: Hill coefficient. ST range: *Stimulus* term range
RWS: Range width of *Stimulus* term. NRWS: Normalized range width of *Stimulus* term.

variability in p53 pulse size increases, the probability of the apoptosis induction curve changes from sigmoidal to hyperbolic. As the cooperativity of PUMA expression by p53 increases, the rigor of the cell fate decision is more disrupted. Among the three types of pulse variability, pulse height variability was the most influential on perturbation because the cooperativity in PUMA expression amplified the variability in stimulus.

In the current study, we set the Hill coefficient of PUMA expression by p53 as 2.0 by default, following the in vitro experiment which showed that p53 binding to DNA has a Hill coefficient of 1.8[30]; however, equation (7) in Table 1 for the PUMA expression by p53 is a simple modeling that, in reality, includes many complex processes. Thus, not only

cooperative binding of p53 to the promoter of the PUMA gene but also many other transcription and translation processes, such as chromatin remodeling or mRNA transport from the nucleus to cytoplasm, are included in the *Stimulus* term. Any factors which influence transcription and translation processes may change the cooperativity of gene expression by p53. Thus, it is possible that cells have various mechanisms to regulate the rigor of cell fate decision by controlling the cooperativity of gene expression by p53.

The suggestion of Sun et al. (2009) and the current work on the influence of cooperativity of the PUMA expression by p53 on the rigor of cell fate decision need to be verified experimentally. For this, firstly, a mutant and/or modified p53 that enhances the expression of PUMA with different levels of cooperativity will be required. Also, cells should be prepared which can stably express such types of p53 after DNA damage. Alternatively, a method to control the cooperativity of the gene expression by p53 could be used to verify our suggestion. Secondly, cells should be damaged by gamma ray radiation at different intensities to induce different numbers of p53 pulses. Finally, the relationship between the number of p53 pulses and the ratio of apoptotic cells should be examined. Using this type of experiment, experimental evidence will be obtained of the relationship between the rigor of the cell fate decision and the cooperativity of gene expression by p53. To accurately count the number of p53 pulses in individual cells, single cell measurements as in time-lapse microscopy are thought to be suitable, as indicated in Lahav et al. (2004).

Although we limited ourselves to the p53 pulse counting mechanism of the Bax activation switch, other mechanisms are also possible. For example, downstream of the Bax activation switch, there exists a caspase cascade[37]. It is thought that because of the existence of a positive feedback loop in the caspase cascade, caspase-3 activation occurs in an all-or-none irreversible manner, similarly to the Bax activation switch[38]. Although PUMA is the main transcriptional target of p53 in various tissues[26–28], p53 is known to enhance the expression of Apaf-1 modestly[25]. Apaf-1 is known to form a complex with cytochrome c and to activate the caspase cascade[37]. Pulse-like concentration changes of p53 may influence Apaf-1 concentration and subsequent caspase cascade activation; therefore, the caspase cascade may also count the number of p53 pulses. Since the two counting mechanisms are not mutually exclusive, both the Bax activation switch and caspase cascade may count the number of p53 pulses and decide the cell fate; however, even if the caspase cascade can count the number of p53 pulses, the influence of the cooperativity of gene expression by p53 is still thought to be important for the rigor of the cell fate decision, as indicated in the current study. The current study sheds light on the probabilistic nature of the cell fate decision, which may make cells fragile; however, homeostasis or the health of our tissues and organs may be ensured by higher order systems such as the immune system.

Acknowledgements

This work was partly supported by a Grant-in-Aid for Scientific Research on Innovative Areas “Molecular Science of Fluctuations toward Biological Functions”, by Research and Development of the Next-Generation Integrated Simulation of Living Matter of MEXT, and by the Global COE Program “Formation of a strategic base for biodiversity and evolutionary research: from genome to ecosystem” of MEXT.

Conflict of interest

There are no conflicts of interest.

Contributors

Y. M. designed and performed the research and analyzed data; and Y. M. and S. T. wrote the paper.

References

1. Aylon, Y. & Oren, M. Living with p53, dying of p53. *Cell* **130**, 597–600 (2007).
2. Batchelor, E., Loewer, A. & Lahav, G. The ups and downs of p53: understanding protein dynamics in single cells. *Nat. Rev. Cancer* **9**, 371–377 (2009).
3. Vousden, K. H. & Lane, D. P. p53 in health and disease. *Nat. Rev. Mol. Cell Biol.* **8**, 275–283 (2007).
4. Adams, J. M. & Cory, S. The Bcl-2 apoptotic switch in cancer development and therapy. *Oncogene* **26**,1324–1337 (2007).
5. Cotter, T. G. Apoptosis and cancer: the genesis of a research field. *Nat. Rev. Cancer* **9**, 501–507 (2009).
6. Mattson, M. P. Apoptosis in neurodegenerative disorders. *Nat. Rev. Mol. Cell Biol.* **1**, 120–129 (2000).
7. Vogelstein, B., Lane, D. & Levine, A. J. Surfing the p53 network. *Nature* **408**, 307–310 (2000).
8. Batchelor, E., Mock, C. S., Bhan, I., Loewer, A. & Lahav, G. Recurrent initiation: a mechanism for triggering p53 pulses in response to DNA damage. *Mol. Cell* **30**, 277–289 (2008).
9. Geva-Zatorsky, N., Rosenfeld, N., Itzkovitz, S., Milo, R., Sigal, A., Dekel, E., Yarnitzky, T., Liron, Y., Polak, P., Lahav, G. & Alon, U. Oscillations and variability in the p53 system. *Mol. Syst. Biol.* **2**, 0033 (2006).
10. Lahav, G., Rosenfeld, N., Sigal, A., Geva-Zatorsky, N., Levine, A. J., Elowitz, M. B. & Alon, U. Dynamics of the p53-Mdm2 feedback loop in individual cells. *Nat. Genet.* **36**, 147–150 (2004).
11. Loewer, A., Batchelor, E., Gaglia, G. & Lahav, G. Basal dynamics of p53 reveal transcriptionally attenuated pulses in cycling cells. *Cell* **142**, 89–100 (2010).
12. Ramalingam, S., Honkanen, P., Young, L., Shimura, T., Austin, J., Steeg, P. S. & Nishizuka, S. Quantitative assessment of the p53-Mdm2 feedback loop using protein lysate microarrays. *Cancer Res.* **67**, 6247–6252 (2007).
13. Tyson, J. J. Monitoring p53’s pulse. *Nat. Genet.* **36**, 113–114 (2004).
14. Hamada, H., Tashima, Y., Kisaka, Y., Iwamoto, K., Hanai, T., Eguchi, Y. & Okamoto, M. Sophisticated framework between cell cycle arrest and apoptosis induction based on p53 dynamics. *PLoS One* **4**, e4795 (2009).
15. Iwamoto, K., Hamada, H., Eguchi, Y. & Okamoto, M. Mathematical modeling of cell cycle regulation in response to DNA

damage: exploring mechanisms of cell-fate determination. *Biosystems* **103**, 384–391 (2011).
16. Sun, T., Chen, C., Wu, Y., Zhang, S., Cui, J. & Shen, P. Modeling the role of p53 pulses in DNA damage-induced cell death decision. *BMC Bioinformatics* **10**, 190 (2009).
17. Wee, K. B., Surana, U. & Aguda, B. D. Oscillations of the p53-Akt network: implications on cell survival and death. *PLoS One* **4**, e4407 (2009).
18. Zhang, T., Brazhnik, P. & Tyson, J. J. Exploring mechanisms of the DNA-damage response: p53 pulses and their possible relevance to apoptosis. *Cell Cycle* **6**, 85–94 (2007).
19. Zhang, T., Brazhnik, P. & Tyson, J. J. Computational analysis of dynamical responses to the intrinsic pathway of programmed cell death. *Biophys. J.* **97**, 415–434 (2009).
20. Zhang, X. P., Liu, F., Cheng, Z. & Wang, W. Cell fate decision mediated by p53 pulses. *Proc. Natl. Acad. Sci. USA* **106**, 12245–12250 (2009).
21. Zhang, X. P., Liu, F. & Wang, W. Coordination between cell cycle progression and cell fate decision by the p53 and E2F1 pathways in response to DNA damage. *J. Biol. Chem.* **285**, 31571–31580 (2010).
22. Haupt, S., Berger, M., Goldberg, Z. & Haupt, Y. Apoptosis — the p53 network. *J. Cell Sci.* **116**, 4077–4085 (2003).
23. Brenner, D. & Mak, T. W. Mitochondrial cell death effectors. *Curr. Opin. Cell Biol.* **21**, 871–877 (2009).
24. Youle, R. J. & Strasser, A. The BCL-2 protein family: opposing activities that mediate cell death. *Nat. Rev. Mol. Cell Biol.* **9**, 47–59 (2008).
25. Yu, J. & Zhang, L. The transcriptional targets of p53 in apoptosis control. *Biochem. Biophys. Res. Commun.* **331**, 851–858 (2005).
26. Nakano, K. & Vousden, K. H. PUMA, a novel proapoptotic gene, is induced by p53. *Mol. Cell* **7**, 683–694 (2001).
27. Villunger, A., Michalak, E. M., Coultas, L., Mullauer, F., Bock, G., Ausserlechner, M. J., Adams, J. M. & Strasser, A. p53- and drug-induced apoptotic responses mediated by BH3-only proteins puma and noxa. *Science* **302**, 1036–1038 (2003).
28. Yu, J., Zhang, L., Hwang, P. M., Kinzler, K. W. & Vogelstein, B. PUMA induces the rapid apoptosis of colorectal cancer cells. *Mol. Cell* **7**, 673–682 (2001).
29. Balagurumoorthy, P., Sakamoto, H., Lewis, M. S., Zambrano, N., Clore, G. M., Gronenborn, A. M., Appella, E. & Harrington, R. E. Four p53 DNA-binding domain peptides bind natural p53-response elements and bend the DNA. *Proc. Natl. Acad. Sci. USA* **92**, 8591–8595 (1995).
30. Weinberg, R. L., Veprintsev, D. B. & Fersht, A. R. Cooperative binding of tetrameric p53 to DNA. *J. Mol. Biol.* **341**, 1145–1159 (2004).
31. Chen, C., Cui, J., Lu H., Wang R., Zhang, S. & Shen, P. Modeling of the role of a Bax-activation switch in the mitochondrial apoptosis decision. *Biophys. J.* **92**, 4304–4315 (2007).
32. Cui, J., Chen, C., Lu, H., Sun, T. & Shen, P. Two independent positive feedbacks and bistability in the Bcl-2 apoptotic switch. *PLoS One* **3**, e1469 (2008).
33. Sun, T., Lin, X., Wei, Y., Xu, Y. & Shen, P. Evaluating bistability of Bax activation switch. *FEBS Lett.* **584**, 954–960 (2010).
34. Albeck, J. G., Burke, J. M., Aldridge, B. B., Zhang, M., Lauffenburger, D. A. & Sorger, P. K. Quantitative analysis of pathways controlling extrinsic apoptosis in single cells. *Mol. Cell* **30**, 11–25 (2008).
35. Vaughan, A. T., Betti, C. J. & Villalobos, M. J. Surviving apoptosis. *Apoptosis* **7**, 173–177 (2002).
36. Tyson, J. J. Another turn for p53. *Mol. Syst. Biol.* **2**, 0032 (2006).
37. Slee, E. A., Harte, M. T., Kluck, R. M., Wolf, B. B., Casiano, C. A., Newmeyer, D. D., Wang, H. G., Reed, J. C., Nicholson, D. W., Alnemri, E. S., Green, D. R. & Martin, S. J. Ordering the cytochrome c-initiated caspase cascade: hierarchical activation of caspases-2, -3, -6, -7, -8, and -10 in a caspase-9-dependent manner. *J. Cell Biol.* **144**, 281–292 (1999).
38. Legewie, S., Bluthgen, N. & Herzel, H. Mathematical modeling identifies inhibitors of apoptosis as mediators of positive feedback and bistability. *PLoS Comput. Biol.* **2**, e120 (2006).